

GSJ: Volume 13, Issue 11, November 2025, Online: ISSN 2320-9186 www.globalscientificjournal.com

SUSTAINABLE DYE REMOVAL : VALORISATION OF CYPERUS ESCULENTUS AGRICULTURAL WASTE FOR WASTEWATER TREATMENT

Okere, K.C.*, Prof Njoku, V.O., Dr. Duru, C.E., Chukwu, F.O. Department of Chemistry, Imo State University, Owerri. Correspondence should be addressed to kevin_chinaka@yahoo.com

ABSTRACT

Industrial dyes pose serious ecological and health risks due to their toxicity and persistence in aquatic environments. This study evaluated the efficacy of Cyperus esculentus (CE) biomass as a low-cost biosorbent for removing methylene blue (MB) from aqueous solutions. CE nuts were washed, oven-dried, ground and sieved (1–2 mm). Batch experiments (4.0 g CE with 100 mL MB; initial concentrations 25–300 mg· L⁻¹) were conducted with agitation (150 rpm); samples were taken over 5–180 min to study contact time and kinetics. The effects of pH (3-10) and temperature (308-323 K) on adsorption were examined; equilibrium isotherms were obtained at ≈ 303 K. SEM imaging revealed a rough, porous surface with cavities favorable for adsorption, and FTIR spectra showed shifts and disappearance of functional-group bands after MB uptake, indicating interactions between MB and CE surface chemistry. Adsorption was rapid initially, then slowed to equilibrium; uptake increased with solution pH and with temperature, suggesting enhanced electrostatic attraction at higher pH and an endothermic process. Kinetic analysis showed the pseudo-second-order model best described the data (high R²; q_e,cal ≈ q_e,exp), implicating chemisorption/strong binding mechanisms. Equilibrium data fit the Freundlich model best (R² = 0.9778), indicating multilayer adsorption on a heterogeneous surface; Langmuir q_m was 1.77 mg·g⁻¹. Thermodynamic parameters indicated spontaneous, endothermic and favorable adsorption $(\Delta G^{\circ} < 0; \Delta H^{\circ} > 0; \Delta S^{\circ} > 0)$. Overall, CE is a promising, low-cost biosorbent for MB removal from wastewater.

Keywords: Industrial Dyes, Wastewater treatment, Valorization, Agricultural Waste.

INTRODUCTION

Dyes are globally known to be essential material in industries such as textiles, cosmetic, plastic and rubber, paper and pulp, printing and ink manufacturing industries. Dye wastewater discharged from these dye stuff industries is one of the major sources of environmental pollution within the aquatic ecosystem and this has become of great concern globally. Wastewater containing Dye stuff is toxic and is potentially carcinogenic, notwithstanding its detrimental impact on aquatic organisms [1-4].

Decolourization of dye-laden effluents has become a very challenging issue, primarily due to the limitations associated with conventional wastewater treatment methods. The treatment of coloured wastewater has been carried out through the application of a variety of physical, chemical and biological methods such as adsorption, coagulation, chemical precipitation, chemical oxidation reverse osmosis, ion exchange and biosorption [5-6]. However, the application of these conventional methods is frequently beset by significant technical and economic drawbacks thereby impeding their applicability [7-9].

Among these methods, biosorption has emerged as a highly effective method with positive prospects for mitigating the limitations of conventional methods in removing dyes from industrial wastewater. Biosorption is the process of uptake of solute (metal or non-metal species) using materials of biological origin whether living or non-living [10-11]. Couple of years ago researchers have shown great interest in studying the applicability of biosorption in treating wastewater and this comes from its many advantages such as treating wastewater with large amount of dyestuff, use of low-cost adsorbents and its minimal operational difficulties. Considering this, researchers are increasingly exploring the use of various materials as potential adsorbents for the removal of dyes and other pollutants from their aqueous solution. Materials such as Pomelo fruit Peel [12], Paenibacillus Mucerans [13], Maize Silk [14], Groundnut Shell and Sorghumttusk, [15] Cocoa Pod Husk [16]. Dyes are typically recalcitrant and exhibit poor degradability and tend to persist in the environment due to their resistance to natural degradation processes therefore, dyestuff wastewater is fraught with major difficulties and so, present a lot of difficulties in the treatment of dyestuff wastewater [17]. Regulations, world over, are pushing for drastic reduction of synthetic dyes in industrial effluents before discharge. Methylene blue is among the most used dyed in the textile industry and has been reported to cause accelerated heart rate, shock, Hemzbody formation, cynanosis, Quadriplegia, Tissue necrosis, and eye burns resulting to eye damage when humans and other animals are in contact with MB due to uncontrolled exposure [18]

The present work explores the potential of using *Cyperus Esculentus* (CE) as an adsorbent for the effective removal of Methylene Blue (MB) from aqueous solutions. The effect of contact time and initial concentration, pH of dye solution and temperature on the adsorption of MB onto CE were examined. The study also investigated the adsorption isotherms, Kinetic and thermodynamics data to elucidate the adsorption process.

MATERIALS AND METHOD

Preparation of Biosorbent

Preparation of biosorbent. The cyperus esculentus, nuts locally called Tiger nut were procured locally. The Cyperus Esculentus (CE) nuts were thoroughly washed with tap water to remove dirt and other adhering materials. The CE nuts were further washed repeatedly with distilled water. The CE nuts where oven dried at 85°C until constant weight was attained. The oven dried sample was subjected to grinding using a domestic mechanical grinder and subsequently sieved to obtain a particle size fraction of 1-2mm and then store in an air tight container for further use.

Preparation of Dye Solution

The dye utilized in this study is of commercial grade, sourced from a local vendor in Port Harcourt, Nigeria. The dye was used without further purification. A stock solution of 1000mg/L was prepared by dissolving 1g of Methylene Blue (MB) in 1L of distilled water. Stock solution was later diluted to required experimental solution concentrations. This dye is used based on its widespread industrial application, adsorptive characteristics and toxicological implications. The molecular structure and general properties of methylene blue are displayed and summarized in table 1, respectively.

Table 1: Some physical and chemical properties of Methylene Blue

Chemical name	Methylene blue
Synonyms/commercial names	Basic blue 9; Swiss blue, Chromosmon, Methylthioninium
	Chloride, Methylthionine Chloride
UPAC names	3,7-Bis (dimethylamino) phenolthiazin-5-ium chloride
Molecular formular	$C_{16}H_{18}CIN_3S$
Formula weight	319.852g/mol

SURFACE AND FUNCTIONAL GROUP CHARACTERIZATION OF CE

The cyperus esculentus chaff was subjected to surface morphology characterization using Scanning Election Microscope (SEM) model JSM-5600LV and Fourier Transformer Infrared (FTIR) model carry -630, an Agilent Fourier Transformer Infrared Spectrophotometer. Using KBr disk method and the FTIR spectrum was recorded in the range of 400-4000cm⁻¹. The surface morphology and possible functional groups in CE that may participate in the adsorption process were characterized.

Batch Biosorption Studies

Batch biosorption equilibrium experiments were conducted to investigate the effect of contact time and initial concentration, pH and temperature on the adsorption of MB onto CE. The experiments were performed in 150ml stoppered conical flasks where 4g of CE was mixed with 100ml of MB solution of known ranges of concentration (25-300mg/L. The mixture was agitated at a constant rate of 150rpm in a water-bath shaker at 30°C. The effect of contact time and initial dye concentration were studied by withdrawing samples at predetermined time intervals (5-180min) and analyzing them using UV spectrophotometer to determine the final MB concentrations. The influence of contact time and initial concentration was evaluated over 25-300mg/L consentration range for predetermine time intervals (5-180 min). The effect of pH was examined by adjusting the dye solution pH to 3-10 using 0.1M HCI and 0.1M NaOH and then contacting 4g of CE with a constant dye concentration of 200mg/L at 30°C. The effect of temperature on the adsorption of MB molecules onto CE was studied over a range of 35-50°C maintaining a constant dye concentration of 200mg/L.

The dye uptake capacity at equilibrium and time t was calculated using equations 1 and 2

$$q_e = \left(\frac{C_o - C_e}{M}\right)V\tag{1}$$

$$q_{t} = \left(\frac{C_{o} - C_{t}}{m}\right) V \tag{2}$$

Where q_e (mgg⁻¹) and q_t (mgg⁻¹) are the amount of dye adsorbed at equilibrium and time t respectively. C_o (mgL⁻¹), C_e (mgL⁻¹) and C_t (mgL⁻¹) are the initial MB concentration, MB concentration at time t and MB concentration at equilibrium. m(g) is the mass of CE biomass used of at time t and equilibrium respectively. The percentage removal was determined by using equation (3).

$$R = \left(\frac{C_o - C_e}{C_o}\right) x \ 100. \tag{3}$$

However, each experiment was performed three times, and the mean values are presented.

Results and Discussion

Surface Characterization of CE

In this study, the surface morphology of CE was examined using Scanning election microscope (SEM). The SEM micrograph of CE before adsorption at 150,000 magnifications is shown in figure 1 highlighting the biosorbents surface characteristics. The micrograph shows the presence of unevenly distributed cavities on rough surface of CE. These cavities on the porous surface of the biosorbent provided sites for the adsorption of MB molecules.

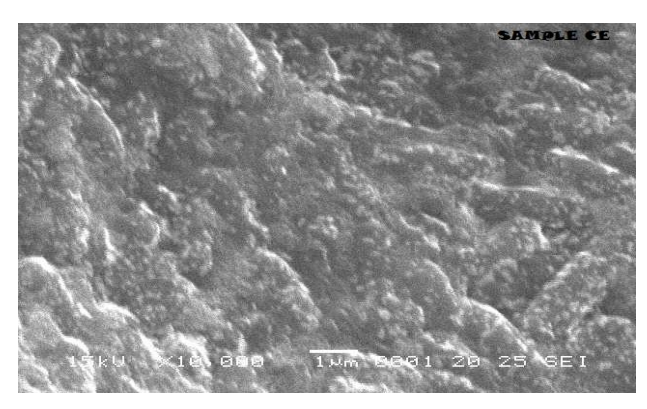


Figure 1: SEM micrograph of Cyperus esculentus (CE)

The Fourier transform infrared (FTIR) speetra of CE before and after adsorption of MB molecules are shown in figures 2 and 3 respectively. The surface functional groups of CE before adsorption of MB showed bands at 3312cm⁻¹ attributed to normal polymeric OH stretching of alcohol, while the bands at 2851cm⁻¹ and 2818cm⁻¹ correspond to NH amine symmetric stretching and C-H a symmetric respectively. The band at 1730m⁻¹ corresponds to strong C-O stretching of alcehydes and ketones. The medium strong absorption bands around 1639cm⁻¹, 1620cm⁻¹ 1544cm⁻¹ and 1238cm⁻¹ were evaluated to correspond to C=C stretching of conjugated Alkene, C = C stretch of ∞, p − unsaturated ketone, N = O of antisymmetric. Stretching of nitro compounds and O − H bonding of carboxylic acids in that order. However, the FT-IR spectra of MB impacted (CEMB) figure 3 showed significant changes in absorption bands shifts from 3313cm⁻¹, 2815cm⁻¹, 2095cm⁻¹, 1639cm⁻¹ 1544cm⁻¹ to 3678cm⁻¹ 2082cm⁻¹, 1620cm⁻¹ 1657cm⁻¹ and 1510cm⁻¹ respectively. While bands at 2918cm⁻¹, 1730cm⁻¹ and 1620cm⁻¹ disappeared after adsorption of MB molecules onto the surface of CE. These shifts and disappearance of bands could be due to the MB molecules interaction with surface chemistry of the adsorbent, (CE) as adsorption process progressed.

Figure 2: The FTIR spectrum of CE

Figure 3: The FTIR spectrum of CEMB

Effect of Adsorbate Solution pH

The influence of adsorbate solution pH on the adsorption process was investigated. Adsorbate solution pH is one of the critical parameters of any adsorption study as it is the key factor that controls surface ionization of adsorbents. pH controls the degree of electrostatic charges transmitted by ionized dye molecules resulting in varing rate of adsorption when the pH is changed [19]. The effect of pH on MB biosorption onto CE was investigated by varying the initial solution pH ranging from 3-10 with fixed initial dye concentration of 200mg/L at 30°C as shown in Figure 4. The biosorptive uptake of MB by CE increased with increase in the adsorbate solution pH. In a low pH region, there could be excessive protonation of the negatively charged active sites on the surface the biosorbent thereby inducing an electrostatic repulsion which further limits the sorptive uptake of MB cations. However, at higher

adsorbate solution pH regions, the surface of adsorbent becomes less protonated giving room for increase in the negatively charged active sites on the surface of the adsorbent hence increasing electrostatic attraction between the positively charged MB cation and the negatively charged active sites resulting in an increase in the MB dye uptake [20-22].

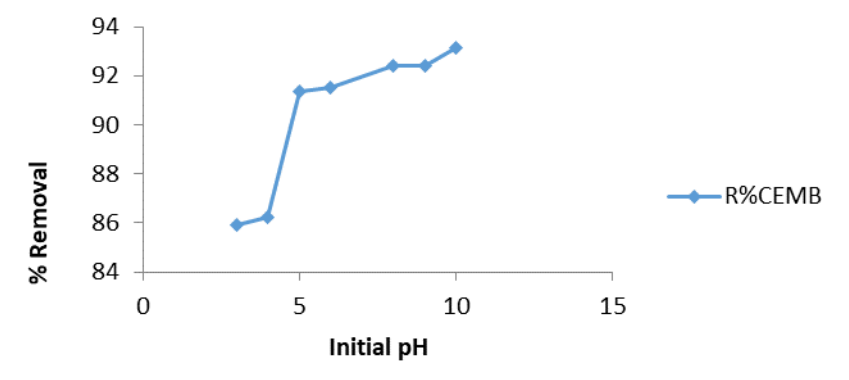


Figure 4: Effect of initial solution pH on percentage removal of MB onto CE

Effect of Temperature

The effect of temperature on the biosorption of MB onto CE was examined using equilibrium experiments to understand the impact of temperature on the adsorption capability of the adsorbent. These experiments were performed at different temperatures ranging from 308, 313, 318 and 323K keeping every other parameters constant (figure 4). The adsorption capacity of CE increased with increase in temperature. This could be attributed to the increase in mobility of MB molecules which is due to the generation of the required energy for MB molecules to surmount the activation barrier and penetrate the adsorbents internal pores more effectively. Similar trends were observed by a couple of adsorption scientists [23,24,18]. The rise in adsorption capacity as temperature increases indicates that the adsorption process is endothermic with respect to the biosorbent used in this study. It has also been reported that for most of the adsorbents used for methylene blue adsorption that adsorption process was endothermic in nature. [18]

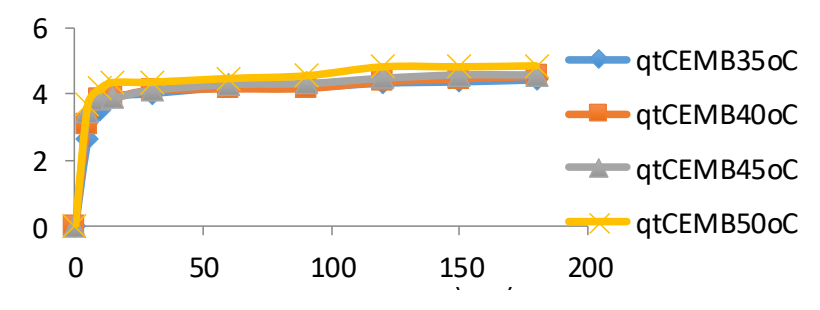


Figure 5. Effect of temperature on the adsorption of MB onto raw CE

Effect of Contact Time and Initial Concentration

Contact time is the measure of the amount of time the adsorbent and adsorbate is placed in contact with each other, while the initial concentration is the measure of amount of dye dissolved in water [19]. The effect of contact time and initial concentration on the biosorption of MB onto CE was investigated by varying the contact time from 5 – 180min and initial concentration from 25-300mg/L. Figure 6 shows the effect of contact time and initial concentration on the adsorption of MB onto CE. As can be seen in figure 6, there was rapid uptake of MB molecules in the initial stages of the adsorption process. This was followed by a slow adsorption rate until equilibriums is attained. The rapid uptake at the initial stage could be due to the abundance of active sites on the larger surface area and the slower sorption rate

was due to saturation of active sites on the surface and further diffusion of MB molecules to active sited on the surface of interior of the CE [25, 26], and [16] all reported similar trends. Adsorption process becomes constant leading to equilibrium probably due to repulsion between MB molecules in the solid and aqueous phase. [15, 25]. The effect of initial concentration on the biosorption of MB onto CE was performed using a wide range of initial concentrations, figure 6 showed that the equilibrium adsorption capacity increased as initial concentration increased. This increase in adsorption capacity could be due to the fact that increase in initial concentration supplied the system with the driving force required to overcome the limitation of mass transfer of dye molecules between the aqueous and solid phases. Furthermore, maximum utilization of available binding sites on the adsorbents lead to increased adsorption capacity at higher initial concentrations. [28, 14].

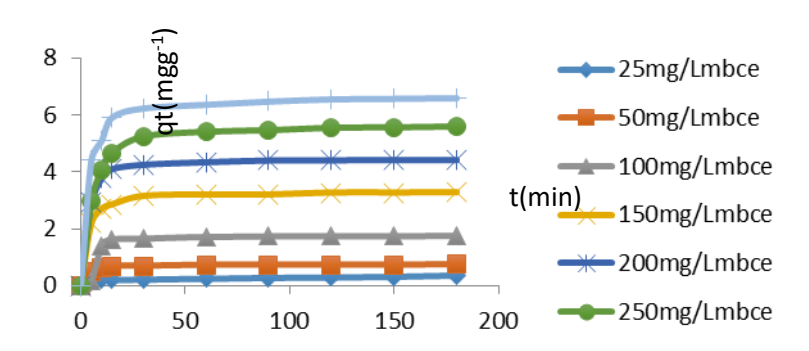


Figure 6. Effect of Contact Time and Initial Concentration on the adsorption of MB onto raw CE

Adsorption Kinetics

Adsorption kinetics predicts the solute (dye) uptake rate which is factored in as one of the essential parameters for the design of industrial adsorption columns.

There are several kinetic models available for predicting the rate and controlling mechanisms of the adsorption process. In this study, five kinetic models were applied to evaluate the experimental data obtained from the adsorption experiment.

These experimental data were fitted into the pseudo-first-order, pseudo-second order. Intraparticle diffusion, Elovich and liquid film diffusion kinetic models.

The linearized pseudo-first-order model is expressed as follows:

$$In(q_e) - q_t - In q_e - K_1 t$$
 (4)

Where $q_s(mgg^{-1})$ is adsorption capacity at equilibrium, $q_t(mgg^{-1})$ is the adsorption

capacity at time t(min), $K_1(min^{-1})$ is rate constant for pseudo-first order (PFO). A plot of $In(q_e - q_t)$ versus t (figure 7) should give a linear relationship from which the values of K₁ and q_e are determined from the slope and intercept respectively.

The linearized form of pseudo-second order (PSO) rate is expressed as equation 5.

$$t/q_t = 1/h_o + 1/q_e t$$
 (5)

Where
$$ho = K_2 q_e^2$$
 (6)

 $q_s(mgg^{-1})$ the amount of adsorbate adsorbed at equilibrium, q_t is the amount of adsorbate adsorbed at time t while K2 is the rate constant for PSO.

A plot of $\frac{t}{q_t}$ vs t (figure 8) gave a slope and interept used to determine the values of q_e and K₂ respectively.

The Elovich kinetic model equation (Low, 1960) expressed as equation (7).

$$q_t = \frac{1}{\beta} \ln(\alpha + \beta) + \frac{1}{\beta} \ln t \tag{7}$$

Where $q_t(mgg^{-1})$ is the adsorption capacity at time t. $\propto (mgg^{-1} \text{ min}^{-1})$ is the initial adsorptive rate while $\beta(gmg^{-1})$ is the desorption constant.

 β is related to extent of surface coverage and activation energy for chemosorption. Parameters β and ∞ can be determined from the slope and intercept of the plot of q_t vs Int (figure 9).

Intraparticle diffusion kinetics model is given by equation (8).

$$q_s = K_{IPD} t^{0.5} + C$$
 (8)

Where $q_t(mgg^{-1})$ is the adsorption capacity at time t, $K_{IPD}(mgg^{-1}mm^{0.5})$ is the Intraparticle diffusion constant while C is the intercept. C is related to the bandary layer thickness.

The intraparticle diffusion plot of q_t vs $t^{0.5}$ is depicted in figure 10. The value of K_{IPD} and C are calculated from the slope and intercept of the plot and shown in table 2.

The liquid film diffusion model equation is given at equation 9.

$$In\left(1 - \frac{q_t}{q_s}\right) = K_{LPD}t + C \tag{9}$$

Where K_{IPD} is the liquid film diffusion constant and C is the intercept

The plot of $\ln\left(1-\frac{q_t}{q_s}\right)$ vs. t is presented in Figure 11.

The value of K_{IPD} is determined from the slope and C from the intercept. The values of the kinetic parameters for all models employed to understand the kinetics and mechanism of the adsorption of MB onto CE are all listed in table 2. The data as present in table 2 show that pseudo-first order (PFO) did not present a good fit for the MB adsorption onto CE given the experimental data it generated. The linear plot of $In\ q_e - q_t$ versus t gave low correlation (R^2) value. Furthermore, the theoretical adsorption capacity q_{ecalc} obtained from the plot varied widely from the experimental adsorption capacity q_{eexpt} which evinced the failure of PFO model to describe the adsorption kinetics of MB onto CE. However, the kinetic data of MB adsorption onto CE was well fitted by pseudo-second order (PSO) kinetic model. The theoretical and experimental adsorption capacities, q_{eexpt} and q_{ecalc} , PSO rate constant, K_2 and the initial adsorption rate ho are listed in table 2 and the plot of $t/q_t vs t$ is presented in figure 8 and this shows that the correlation coefficient (R^2) value is close to unity.

Furthermore, there is a satisfactory agreement between experimental and theoretical q_e values which further confirms that the adsorption of MB onto CE followed PSO. Hence it is safe to postulate that chemisorption played a key role in the adsorption process [29, 30].

postulate that chemisorption played a key role in the adsorption process [29, 30]. The Intraparticle diffusion kinetic model plot of $q_t vs t^{0.5}$ (figure 10) of MB onto Ce showed that the majority of the plot did not pass through origin and the correlation coefficient R^2 values Table 2, are largely less than unity, suggesting that the intraparticle diffusion did not play a significant role in the mechanism governing the adsorptive uptake of MB onto CE.

The Elovich model did not exhibit a good fit to the experimental data (figure 10).

This clearly shows that PSO model is the most prominent kinetic model to describe the kinetics of MB adsorption onto CE as chemosorption. This is due to the correlation coefficient R^2 value (table 2) that are very low and far from unity.

Liquid film diffusion model plot of $\ln \left(1 - \frac{q_t}{q_e}\right) vs t$ (figure 11) for the adsorption of MB onto CE did not produce a straight line from origin. The plot also produced a low correlation

coefficient R² value (table 2) Suggesting that liquid film diffusion model did poorly in appropriately predicting the mechanism of the adsorption of MB onto CE.

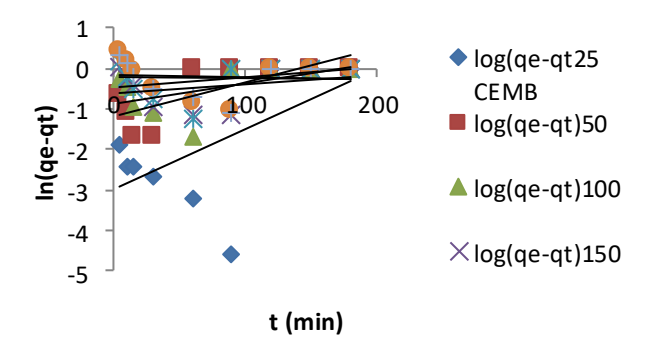
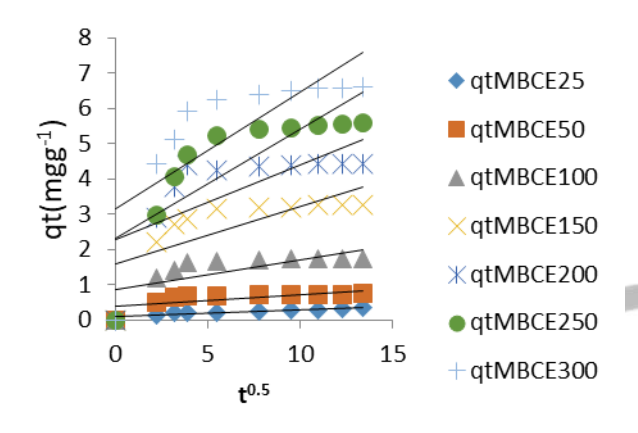


Figure 7: Pseudo-first-order plot for the adsorption of MB onto raw CE at different initial MB concentrations

Figure 8:. Pseudo-second-order plot for the adsorption of MB onto raw CE at different initial MB concentrations



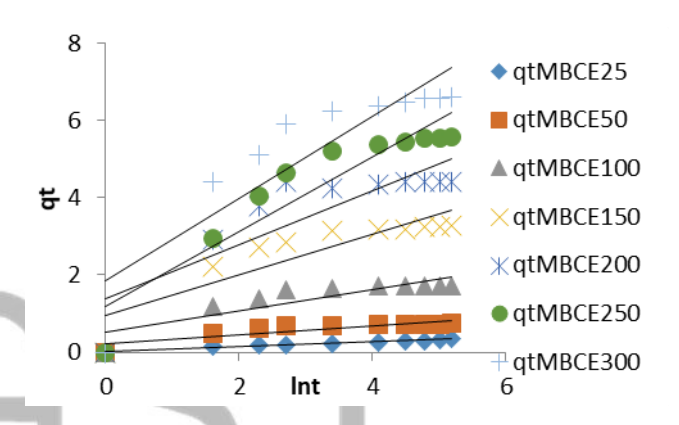


Figure 9: Intraparticle Diffusion Model Plot for adsorption of MA onto CE

Figure 10: Elovich Model Plot for absorption of MB

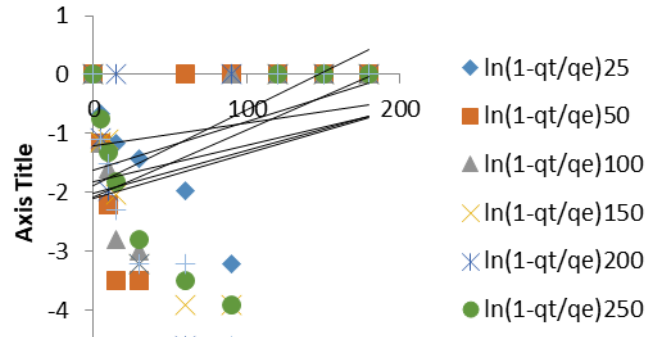


Table 2: Parameters of Different Kinetic and Mechanismt Model of MB adsorption unto CE

Axis Title

Figure	11:	Lıquıd-film	diffusion	kınetic	model	plot for	the a	dsorption	of MB	onto CE	,

MBO	(mg/L)	Pseudo	First Order	PFO	Pseudo	qe	2 nd Order	PSO	Intrapa	ticle diffu	sion	Elovic	h		Liquid	film diffu	sion
Adsorbent	Co (mg/L)	q _e (mg/g)	K₁(1/min)	R ²	q _e (mgg ⁻¹)	Calt mgg ⁻¹)	K ₂ (gmg ⁻² min ⁻¹)	R ²	\mathbf{K}_{IPD}	С	R ²	а	b	R ²	K _{LFD}	С	R ²
CE	25	0.9015×10 ⁻⁴	0.0343	0.3589	0.3569	0.29	0.1864	0.9777	0.020	0.083	0.896	0.093	16.950	0.954	0.003	-1.219	0.058
	50	0.0636	-0.0196	0.5470	0.7369	0.71	0.6030	0.9994	0.034	0.372	0.489	0.843	8.850	0.728	0.012	-1.893	0.322
	100	0.1324	0.0120	0.2936	1.7646	1.73	0.2674	0.9999	0.98	0.811	0.544	1.833	3.610	0.758	0.011	-2.071	0.203
	150	0.2598	-5.067×10 ⁻³	0.7660	3.3102	3.26	0.1320	0.9999	0.161	1.600	0.536	0.899	1.908	0.773	0.007	-2.021	0.084
	200	0.3486	-5.527×10 ⁻³	0.1138	4.2176	4.40	0.6622	0.9867	0.210	2.286	0.478	5.018	1.031	0.722	0.008	-1.633	0.106
	250	0.6790	1.3818×10 ⁻³	0.0059	5.6850	5.53	0.0481	0.9999	0.307	2.325	0.633	3.251	1.031	0.860	0.006	-1.824	0.071
	300	0.6257	6.909×10 ⁻⁴	0.0014	6.6934	6.56	0.0580	1.0000	0.330	3155	0.553	5.207	0.936	0.788	0.007	-2.098	0.088

Adsorption Isotherm Models

Adsorption isotherm describes the correlation between the amount of adsorbate adsorbed and its equilibrium concentration at constant temperature.

Adsorption isotherms afford valuable insights into the optimal utilization of adsorbents, enabling the appropriate theoretical modeling and design of efficient adsorption system [31,32]. Within the framework of this study, the equilibrium adsorption data evaluation was performed using different initial concentrations 25-300mg/L at 303K. The experimental equilibrium data were analysed using five isotherm models, Langmuir, Freundlich, Temkin and Dubinin-Radushkevich models.

Langmuir isotherm model [33] is based on the assumption that adsorption occurs with the existence of monolayer coverage of the adsorbate molecules on the exterior surface of the adsorbent material with a uniform adsorption energy on the surface of adsorbent. The Langmuir isotherm model is mathematically expressed linearly as equation 10.

$$c_e/q_e = \frac{1}{q_m K_L + \frac{C_e}{q_m}} \tag{10}$$

Where

 $q_{\varepsilon}(mgg^{-1})$ is the amount of dye adsorbed at equilibrium, $q_m(mgg^{-1})$ is the monolayer adsorption capacity of the adsorbent, $C_e(mg/L)$ is the equilibrium dye concentration and $K_L(L^3mg^{-1})$ is the Langmuir adsorption constant associated with the free energy of adsorption. q_m and K_L are derived from the slope and intercept of the plot of $C_{\varepsilon}/q_{\varepsilon}$ versus C_e in the context of Langmuir isotherm model [28] the dimensionless separation factor R_L , expressed in equation 11. Provides a widely used indicator for critical insights into the adsorption process.

$$R_L = \frac{1}{1 + K_L C_o} \tag{11}$$

Where $Co(mgL^{-1})$ is the highest initial concentration R_L indicates whether an adsorption process is irreversible if $R_L = O$, favourable if $(0 < R_L 1)$ and unfavourable if $R_L = 1$.

Freundlich Isotherm Model

The Freundlich isotherm model [34] is an empirically based equation that captures characterization of adsorption on heterogeneous surfaces, where the stronger binding sites are occupied preceding the weaker binding sites and attendant decrease in binding affinity. The Freundlich Isotherm equations expressed as follows:

$$Inq_{e} = InK_{F} + \frac{1}{n_{F} InC_{e}}$$
(11)

Where $K_F(mgg^{-1}(mgL^{-1})^{-1/n})$ is the sorption capacity of adsorbent while the dimensionless constant n_F represents the sorption intensity. The values of n_F and K_F are calculated from the slope and intercept of the plot of In q_e vs. InCe respectively. The value of n_F ranges between 1 and 10 and a higher value of n_F suggests better adsorption [18].

Temkin Isotherm Model

The Temkin isotherm model accounts for the indirect interaction between the molecules of the adsorbate. Additionally, Temkin model assumes that the heat of adsorption decreases linearly with the increase in coverage of the adsorbent surface [35, 36]. Temkin isotherm model is linearly expressed as follows:

$$q_e = \frac{RT}{b_T} InK_T + \frac{RT}{b_T} In Ce$$
 (12)

Where R is the universal gas constant (8.314Jmol⁻¹K⁻¹), T(K) is the absolute temperature, $b_T(Jmol^{-1})$ is the Temkin constant related to the heat of adsorption, serving as a key indicator of the adsorbent's adsorption potential (intensity), and $K_T(Lg^{-1})$ is the Temkin constant, related to adsorption capacity.

The linear plot of q_e versus InC_e allows for the determination of b_T and K_T from the scope and intercept respectively.

Dubinin-Radushkevich Isotherm Model

Dubinin-Radushkevich Isotherm Model [37] is a isotherm model that evalutes the characteristic porosity of an adsorbent and elucidates the apparent adsorption energy, thus yielding valuable insights into the adsorption phenonena. The model helps to understand whether the adsorption process is chemisorption or physisorption [12]. Dubinin-Raduschkevich is represented by the following equation (13).

$$In \ q_{\varepsilon} = In \ q_{\Delta R} - \beta \varepsilon^2 \tag{13}$$

Where $q_{DR}(mgg^{-1})$ is the Dubinin-Radushkevich maximum $\beta(mol^2J_2)$ is the activity coefficient related to the mean sorption energy E(KJmol⁻¹). E is determined by using the equation (14)

$$E = \frac{1}{(2\beta)^{0.5}} \tag{14}$$

While ε is the Polanyi potential which is calculated using equation (15).

$$\varepsilon = RT \ln \left(1 + \frac{1}{C_s} \right) \tag{15}$$

Where R(8.314 Jmol⁻K⁻¹) is the universal gas constant T(K) is the temperature. However, the values of β and q_{DR} are obtained from the slope and intercept of the plot a of In q_e versus ε^2 respectively.

The analysis of adsorption isotherm parameters of models employed in this study is very relevant as it helps in developing accurate data that would be used for adsorption design purpose in a larger scale. The linear plots of the five isotherm models are presented in figures 12-16. The values of their distinctive parameters are shown in Table 3. Judging from the correlation coefficient (R^2) values, the adsorption of MB onto CE followed this order for the best fitted isotherm models Freundlich > Temkin> Langmuir>Dubinin-Radushkevich. The values of n_f and K_f (table 4) calculated from the slope and intercept of the linearized Freundlich plot of Inqe versus InCe show that n < 1 which implies a weak adsorption connection between molecules of methylene blue and the adsorbent also indicating a poor adsorption capability [1, 34]. However, the alignment of the correlation coefficient (R^2) with Freundlich model discloses a multilayer adsorption process and the heterogeneity of adsorbent surface of CE.

The Langmuir Model monolayer adsorption capacity q_m was determined to be 1.77mgg⁻¹ as shown in table 3. While the R_L values suggests a favourable adsorption. R_L is a dimensionless Langmuir model which indicates whether an adsorption process is favourable when $0 < R_L < 1$ Linear if $R_L = 1$ and unfavourable if $R_L > 1$.

The Temkin Isotherm model evaluates the effects of indirect adsorbate interactions on adsorption isotherm and assumes that heat of adsorption of adsorbate decreases linearly with increasing surface coverage due to adsorbate -adsorbate interactions.

The Temkin Isotherm parameters b_T and K_T are calculated from the slope and intercept of plot of q_e versus InC_e and values listed in table 4, However, the Temkin Isotherm model inadequately describes the equilibrium data, given the comparatively low R^2 value of 0.8379, which could imply that the isotherm model assumptions could not be entirely credible for the describing the CE-MB adsorption process. The Dubini-Raduschevich Isotherm Model parameters determined from the slope and intercept of the plot of Inq_e versus ε^2 , figure 6 as shown in table 3 indicates that while the Dubini-Raduschevich isotherm model provided some critical perspectives on the adsorption process, the correlation – coefficient (R^2) value of 0.609, that is less than unity. suggests that DRK could not offer a valid fitting for the MB adsorption on CE. However, DRK gives insight into the physical and chemical nature of the adsorption process. The mean free energy ε value was calculated to be <8KJMol implying that physisorption was predominant in the adsorption process [39].

Appraising by the R^2 values presented in table 3. The order of isotherm model fit is confirmed to be Freundlich > Temkin, > Langmuir > Dubinin - Radushkevich. The order suggests that Freundlich model provides the best fit to the experimental data. A comparism of the q_m values determined from this study with q_m values from other studies is presented in table 5.



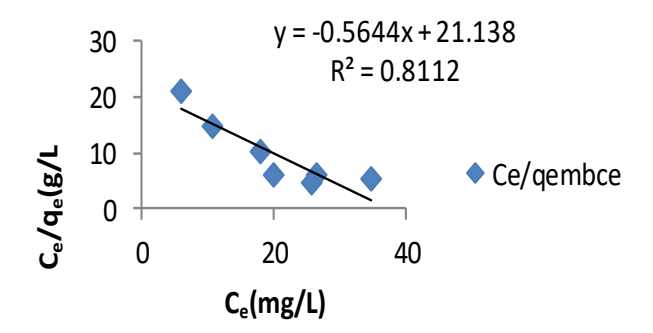


Figure 12: Langmuir adsorption plot of MB onto

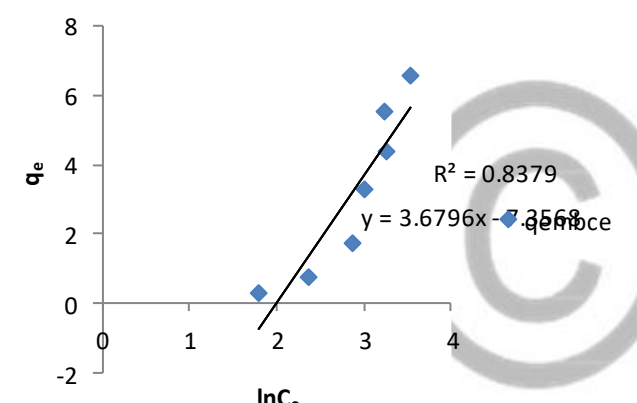


Figure 14: Temkin adsorption plot of MB onto CE

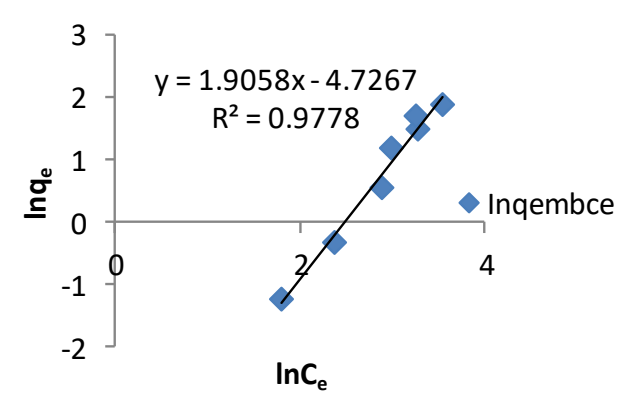


Figure 13: Freundlich adsorption plot of MB onto CE

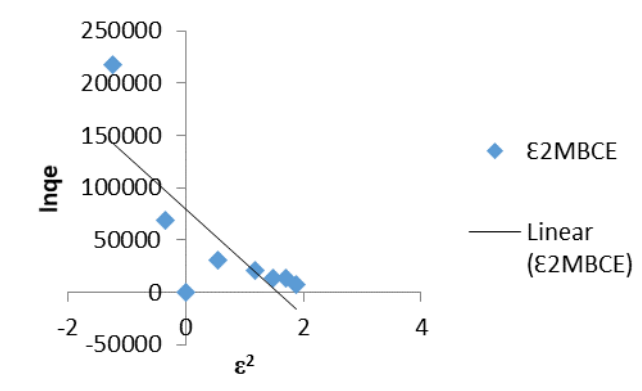


Figure 15: Dubinin-Radushkevich adsorption plot of MB onto CE

Table 4: The parameters of Langmuir, Freundlich, Temkin, Dubinin-Radushkevich and Redlich-Peterson isotherms for the adsorption of MB.

Isotherm Model	CE
Langmuir	
qm (mgg ⁻¹)	1.77
$K_{ m L}$	0.0267
\mathbb{R}^2	0.8112
$R_{ m L}$	0.1427
Freundlich	
$K_F(Lg^{-1})$	8.86×10^{-3}
nF	0.5247
\mathbb{R}^2	0.9778
Temkin	
$K_T(Lg^{-1})$	0.1354
$B_T(mgg^{-1})$	684.62
\mathbb{R}^2	0.8379
b_{T}	3.6796
Dubinin-Radushkevich	
$q_{DKR(mgg}^{-1})$	79819
E (KJmol ⁻¹)	3.14×10^{-3}
$\beta (\text{mol}^2 \text{J}^2)$	50860
R^2	0.609

Table 5: Adsorption capacity of different adsorbents for removal of methylene blue dye

Adsorbent	qm (mg/g)	References
Cyperus esculentus	1.77	(Present study)
Groundnut shell	7.052	[15]
Pinewood AC	5.56	[28]
Rice husk (coir pith carbon)	5.87	[40]
Wheat bran	3.08	[41]
(zeo-FPT) (1:1) biosorbent	0.438	[30]
Zeo-x from Ethiopian Kaolin	0.61	[42]

Adsorption Thermodynamics

Thermodynamics studies give valuable insights into energy variations that drive the adsorption process which is crucial for profiling the adsorption system's thermodynamic behaviour. The thermodynamic behaviour of any adsorption process is studied using the predictions of thermodynamic parameters such as Gibbs free energy (ΔG°), enthalpy (ΔH^{0}) and entropy (ΔS^{0}). The feasibility of adsorption process depends on the outcome of the evaluation of these three parameters ΔG^{0} , ΔH^{0} and ΔS^{0} . These parameters were calculated using equations 15, 16 and 17

$$\Delta G^0 = RTInK_D \tag{15}$$

$$InK_D = \frac{\Delta S^0}{R} - \frac{\Delta H^0}{RT} \tag{16}$$

$$K_D = \frac{C_e}{C_o}$$
 (17)

Where $K_D(Lg^{-1})$ is the thermodynamic equilibrium constant, R (8.314Jmol⁻¹K⁻¹) is the universal good constant and T(K) is the temperature. Values of ΔH^0 and ΔS^0 (Table 6) were calculated from the slope and intercept of Van't Hoff's straight-line plot of InK_D vs $\frac{1}{T_{\Delta}}$ (Figure 17) respectively. The negative value of ΔG^0 (Table 6) predicts that the sorption of MB on CE is spontaneous in nature.

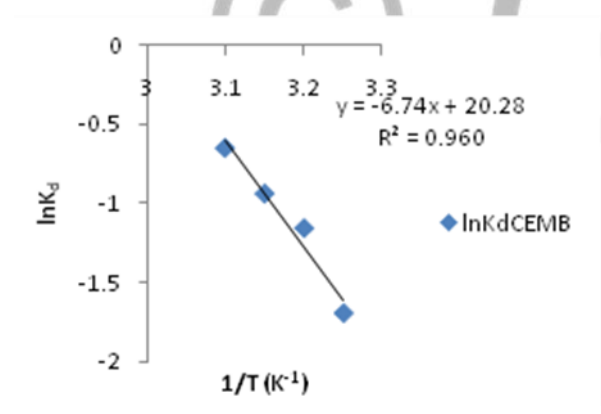


Fig. 17: Van't Hoff plot for the adsorption of MB onto raw CE

Table 6: Thermodynamic parameter for the adsorption of MB onto CE

Adsorbents	Temperature K	$\Delta \mathrm{G}(\mathrm{kg/mol})$	$\Delta H(KJ/mol)$	$\Delta \mathrm{SJK^{\text{-}1}mol^{\text{-}1}}$
CE	308	-51.90	+56.04	+168.69
	313	-52.74		
	318	-53.59		
	323	-54.43		

Conclusion

In this present work, it was discovered that Cyperus esculentus (CE) is a suitable biosorbent for the removal of methylene blue (MB) from aqueous solution. The Freundlich Isotherm model has the best correlation coefficient of all isotherm models used for the adsorption of MB onto CE. The pseudo-second-order kinetics was successfully applied to experimental data. The thermodynamic examination of the adsorption data has indicated that the adsorption process of MB onto Ce at 308K, 313K, 318K and 323K, is spontaneous, endothermic and favourable.

References

- [1] Al-Asadi, S.T., Musa, Z.H., Al-Qaim, F.F., Kamyab, H., Al-Saedi, H.F.S., Deyab, I.F. and Kadhim, N.J. (2025). A comprehensive review of methylene blue dye adsorption on activated carbon from edible fruit seeds: A case study on kinetics and adsorption models carbon trends 20 100507.
- [2] Oladoye, P.O. Ajiboye, T.O. Omotola, E.O. and Oyewola (2022). Methylene blue dye toxility and potential elimination technology from wastewater. Results Eng. (16).
- [3] Alhardy, N.F., Almutari, R.S. and Mohamed, N.A. (2021). Adsorption behaviour of methylene blue dye by Novel Crosslinked O-CM-Chitosan Hydrogel in aqueous solution: kinetics, isotherm and thermodynamics. Polymers 13, 3659.
- [4] Lin, K. and Zhao H. (2022). The impact of green finance on the ecologicalization of urban industrial structure Based on GMM of dynamic panel system. J. Artif. Intell. Technol (2) 123-129.
- [5] Manavi, N., Kazemi, A.S. and Bonakdarpour, B. (2017). The development of aerobic granules from conventional activated sludge under anaerobic-aerobic cycles and their adaptation for treatment of dyeing wastewater. Chem. Eng. J. (312) 375-384.
- [6] Chacko J.T. and subramaniam K. (2011) Emymatic degradation of azo dyes A review. Int. J. Environ. Sci 1 (6) 1250 1260.

- [7] Dimbo, G., Abewa, M. Adino E., Mengistu, A., Takele, T. Oro, A. and Rangaraju, M. (2024) Methylene blue adsorption from aqueous solution using activated carbon of spathodea campanulas a results Eng (21) 10191
- [9] Njoku, V.O., Foo, K.Y. and Hameed, B.H. (2013). Microwave assisted preparation hull activated carbon and its application for the adsorptive removal of 2, 4-dichlorophenoxyacetic acid. Chemical Engineering Journal 215-216, 383 388.
- [10] Figueria, M.M., Volesky, B., Azarian, K. and Cimmelli, V.S.T (2000) Biosorption column performance with a metal mixture. Environ. Sci. Technol. 4320-4326.
- [11] Volesky, B. (2001). Biosorption for the next century hydrometa Uurgy 59 (2-3) 203 216, 59 (2-3) 203 216.
- [12] Dinh, V-P., Huynh, T-D-T., Le, H.M., Nguyen, V.∆., Dao, V.-A. Hung, Q.N. Tuyen, A. L., Lee, Y. J., Nguyen, T. D. and Tan L.V. (2019) Insight into the adsorption mechanism of methylene blue and chromium (III) from aqueous solution onto pommels fruit peel RSC. Adv. (9) 25847-25860.
- [13] Colak, F., Atar, N. and Olgun, A. (2009). Biosorption of acidic dyes from aqueous solution by Paenibacillus Macerans: Kinetic, Thermodynamic and Equilibrium Studies Chemical Engineering Journal Ibo: 1 122 130.
- [14] Miraboutalebi, S. M., N. Kouzad, S.K., Peydayesh, M., Allahgholi, N., Vofajoo, L. and Mckay, G. (2017) Mellylene blue adsorption via maize silk powder: Kinetic, equilibrium, Thermodynamic studies and residual error analysis process Saf. Environ. Prof. (106) 191-202.
- [15] Hammari, A. M., Abubakar H., Misau, M.I., Aroke, U.O. and Hamza, U.D. (2020) Adsorption equilibrium and kinetic studies of methylene blue dye using groundnut shell and sorghum husk biosorbent. *Journal of Environmental Bioremediation and Toxicology* (3) 2 32-39.
- [16] Njoku, V.O., Ajuk, A.A., Oguzie, E.E. and Ejike, E.N. (2012). Biosorption of Cd(ii) from aqueous solution by cocoa pod husk biomass: Equilibrium, kinetics, and themodynamic studies, separation science and technology 4 7:5, 753 761.
- [17] Weber, W.J. and Morris J.C. (1964). Pargamon Press New York.
- [18] Corda, N. C. and Kini, M.S. (2018). A review of adsorption of cationic dyes using activated carbon. MATEC web of conferences (144) 02022.
- [18] Hasani, N., Selimi T., Mele, A., Thaci, V., Halili, J., Berisha, A. and Sadiku, M. (2022). Theoreitical Equilibrium, Kinetics and Thermodynamic investigations of methylene blue adsorption onto Lignite coal. Molecules (27) 1856-1874.
- [19] Katheresan, V., Kansedo, J. and Lau, S.Y. (2018). Efficiency of various recent wastewater dye removal methods. A review. *Journal of Environmental chemical engineering* (6) 4676-4697.

- [19] Yu, L. and Luo, Y.-M. (2014). The adsorption mechanisms of anionic and cationic dyes by Jerusalem artichoke stalkbased mesoporous activated carbon J. Environ. Chem. Eng. (2) 220-229.
- [20] Chiou, M.S. and Chuang, G.S., (2006) Competitive adsorption of dye metanil yellow and RB15 in acidic solutions on and chemically corss-linked chitosan beads. Chemosphere (62) 731-740.
- [21] Twardowska, T., Hea, A.F. and Kettrup, W.J. (2003) Solid waste Assessment, Monitoring and Remediation: Gulf Professioal Publishing ISBN 0080443214.
- [22] Nithyalakshmi, B. and Saraswathi, R. (2021). Removal of colorants from wastewater using biochar derived from leaf waste. Biomass convers. Biorefinery 1303 1-17.
- [23] Mahmoodi, N.M., Arami, M., Bahrami, H. and Khorramfar, S. (2010). Novel Insorbent (Canola Hull): Surface Characterization and Dye Removal ability at different cationic dye Concentrations. Desalination 264, 134 142.
- [24] Ebrahimian, A., Pirabazari, A., Saberikhah, E., Badrouh, M. and Emami, S. (2014). Alkali treated fournanate tea waste as an efficient adsorbent for methylene blue absorption from aqueous solution. Water Resources and Industry 6, 64 80.
- [25] Hazza, R. and Hussein, M (2015) Adsorption of anconic dye from aqueous solution onto activated carbon prepared from olive stones. Environmental technology and Innovation (4) 36-51.
- [26] Regti, A., Laamari, M.R., Striba, S.E. and El Haddad, M. (2017). iotential use of activated cartbon drived from under alkaline conditions Persea Specia for removing cationic dye from wastewaters. J. Assoc. arab Univ. Basic appl. Sci. (24) 10-18.
- [27] Kandisa, R.V., Saibaba, K.V., Shaik K.B. and Gopinadh, R. (2021). Studies on effects of adsorption parameters for the methylene blue removal by using low-cost adsorbent RASAYAN J. Chem. 14, 2. 1528 1533.
- [28] Salleh, M.A.M., Mahmood, D.K., Karim, W.A.W. A and Idris, A. (2011) catwnic and anionic dye adsorption by agricultural solid wasters: A comprehensive review. Desalination (280) 1-13.
- [29] Belachew, N. and Hinsene, H. (2022). Preparation fo zeolite 4A for adsoptive removal of methylene blue: optiminzation,. Kinetics, isotherm, and mechanism study. Silicon (14) 1629-1641.
- [30] Alhogbi, B.G. and Al Balawi G.S. (2023). An investigation fo a natural biosorbent for removing methylene blue dye from aqueous solution. Molecules (28) 2785-2800.
- [31] Foo, K. and Hameed, B. (2012). Adsorption Characteristics of industrial solid waste derived activated carbon, prepared by microwaved heating for methylene blue. Fuel Processing Technology 99, 103 109.

- [32] Boukhemkhem, A. and Rida, K. (2017). Improvement of adsorption capacity of methylene blue onto modified Tamazert Kaolin. Adsorption Science and Technology (35) (9 10), 753 773.
- [33] Lamgmuir, I. (1918). The adsorption of gases on plane surfaces of glass, mica and platinum. J.Am. Chem. Soc. (40) 1361-1403.
- [34] Freundlich, H.M (1906) Uber die adsorption in LÖsungen. C. Phys. Chem. (57) 385-470.
- [35] Dada, A.O., Ojediran, J.O. and Olalekan, A.P. (2013) Sorption of Pb²⁺ from aqueous solution unto modified rice husk: Isotherms studies. Advances in physical chemcistry (2) 1-6.
- [36] Temkin, M.J. and Pyzhev., V. (1940) Kinetics of ammonia synthesis on promoted iron catalysis. Acra. Physiochem USSR (12) 327-356.
- [37] Dubinin, M.M. and Radushkavich, L.V. (1947) Proe. Acad. Sci USSR (55) 331.
- [38] Jawed, A.H., Mallah, S.H and Mastuli, M.S. (2018). Adsorption behaviour of methylene blue on acid-treated rubber (Hevea brasiliensis) Desaln. Water Treat (124) 297-307.
- [39] Chabani, A., Amrane, A. and Bensmaili A. (2006) Kinetic modeline of the adsorption of nitrates by ion exchange resin. Chem. Eng. J. (125) 111-117.
- [40] Kavitha, D. and Namasivayam, C. (2007). Experimental and Kinetics studies on methylene blue adsorption by coirpith carbon. Bioresources Technology 98, 1 14 21.
- [41] Hamdaoui, O. and Chiha, M. (2007). Removal of methylene blue from aqueous solution by what Bran, Acta Chim Slov (54) 407 418.
- [42] Mulushewa, Z., Dinbore, W.T. and Ayele, (2021). Removal of methylene blue from textile waste water using Karlin and Zeolittl-x Synthesized from Ethopian Kaolin Enurm. Anal. Health Toxicole (36) e 2021007.